Chemosphere 263 (2021) 128261

Contents lists available at ScienceDirect

Chemosphere

journal homepage: www.elsevier.com/locate/chemosphere

# Episodic surges in titanium dioxide engineered particle concentrations in surface waters following rainfall events

Md Mahmudun Nabi, Jingjing Wang, Mohammed Baalousha*

*Center for Environmental Nanoscience and Risk, Department of Environmental Health Sciences, Arnold School of Public Health, University of South Carolina, Columbia, SC, USA*

## HIGHLIGHTS

- Quantification of $TiO_2$ engineered particles in urban surface waters.
- Ti/Nb ratio was used to estimate $TiO_2$ engineered particle concentrations in river water.
- Rainfall events convey $TiO_2$ engineered particles to the urban surface waters.
- Elemental ratios in natural Ti-containing particles were characterized on a single particle basis.
- Elemental ratios within natural Ti-containing particles were constant during the sampling period.

## ARTICLE INFO

*Article history:*
Received 30 May 2020
Received in revised form
2 August 2020
Accepted 2 September 2020
Available online 7 September 2020

Handling Editor: Patryk Oleszczuk

*Keywords:*
Titanium dioxide
Engineered particles
Quantification
Multi-element single particle
Urban rivers
Elemental ratios

## ABSTRACT

Quantifying and characterizing engineered particles in environmental systems is key for assessing their risk but remains challenging and requires the distinction between natural and engineered particles. The objective of this study was to characterize and quantify the concentrations of titanium dioxide engineered particles in the Broad River, Columbia, South Carolina, United States during and following rainfall events. The elemental ratio distributions of Ti/Nb, Ti/Fe, and Ti/Al, determined on a single particle basis using inductively coupled plasma-time of flight-mass spectrometry (SP-ICP-TOF-MS), were similar between samples during the different rainfall events, indicating that naturally occurring particles had the same elemental ratios and origin. Therefore, the changes in the Ti/Nb ratios in the bulk water samples were attributed to the introduction of titanium dioxide engineered particles into the Broad River with urban runoff during and following rainfall events. The total concentrations of Ti, Fe, Al, Nb, Ce, and La in the Broad River followed the same trend of rise and fall as the discharge/runoff. The elemental ratios of Ti/Nb were higher (*e.g.,* 330 to 565) than the average crustal values (*e.g.,* 320) and the natural background elemental ratios in surface waters in Columbia, SC (*e.g.,* 266.4 ± 8.9), suggesting contamination with titanium dioxide engineered particles. The concentration of titanium dioxide engineered particles were estimated by mass balance calculations using total titanium concentrations and increases in Ti/Nb ratios above the natural background ratios. The concentrations of titanium dioxide engineered particles in the Broad River varied between 20 and 140 μg $TiO_2$ $L^{-1}$ following rainfall events. The source of titanium dioxide was attributed to urban runoff due to the absence of sewage contamination as indicated by the low size of the gadolinium anomaly. The findings of this study demonstrate that urban runoff is a major source of titanium dioxide engineered particles to urban rivers, which results in episodic high concentrations of titanium dioxide engineered particles, which may pose environmental risks during and following rainfall events. This study also highlights the importance of determining the temporal variations in engineered particle concentrations in surface waters for a more comprehensive risk assessment of engineered particles.



## 1. Introduction

Urban runoff is widely recognized as a major vector of chemicals, including engineered particles (*e.g.,* engineered nanoparticles

* Corresponding author.
*E-mail address:* mbaalous@mailbox.sc.edu (M. Baalousha).

https://doi.org/10.1016/j.chemosphere.2020.128261
0045-6535/

and pigments), to surface waters, and therefore urban runoff has been shown to contribute significantly to the deterioration of surface water quality (Müller et al., 2020). Many studies investigated the release of engineered particles from municipal wastewater treatment plants (Kiser et al., 2009), sewage spills (Loosli et al., 2019), and from sunscreens (Gondikas et al., 2014; Reed et al., 2017) to urban surface waters. However, little attention has been given to the contribution of the built urban environment to the fluxes of engineered particles in urban surface waters, despite the many uses of engineered particles in the urban environment (Baalousha et al., 2016). Titanium dioxide ($TiO_2$) engineered particles are widely used in the urban environment both as pigments (*e.g.*,100–300 nm) in paint and nanosized particles (*e.g.*,1–100 nm) in self-cleaning and photocatalytic surfaces (Baalousha et al., 2016). These uses of $TiO_2$ engineered particles results in their release, and deposition on surfaces in the urban environment (Gohler et al., 2010; Koponen et al., 2011; Nored et al., 2018). During rainfall events, the deposited particles are washed with urban runoff to the receiving surface waters, which is likely to result in high episodic engineered particle concentrations in urban surface waters during and following rainfall events. For instance, a recent environmental fate modeling study suggested that $TiO_2$ engineered nanoparticle concentrations could reach 600–1500 μg $L^{-1}$ in urban rivers impacted by stormwater runoff (Parker and Keller, 2019). Another study reported high concentrations (5–150 μg $L^{-1}$) of $TiO_2$ engineered particles in bridge runoff and in urban rivers dominated by urban runoff (Wang et al., 2020). However, these measurements were a proof of concept of the analytical approach and did not take into account the temporal variability of the measured engineered particle concentrations.

Currently, most available data on engineered particles, including $TiO_2$, concentrations in environmental systems are predicted based on mass flow and environmental fate models (Lützhøft et al., 2015; Mueller and Nowack, 2008). These models estimated that the concentrations of engineered nanoparticles, including $TiO_2$, are likely to be in the ng to low μg $L^{-1}$ range. Nonetheless, a recent modeling study predicted high concentrations (*e.g.*, 619–1490 μg $L^{-1}$) of $TiO_2$ engineered nanoparticles in urban rivers impacted by stormwater (Parker and Keller, 2019). However, these predictions may suffer from significant uncertainties because they are based on modeling approaches that have not been validated against field measurements. Few studies reported the occurrence and the measured concentrations of $TiO_2$ engineered nanoparticles in environmental systems and many of them reported low $TiO_2$ engineered nanoparticle concentrations which are in line with the modeled environmental concentrations (Gondikas et al., 2014, 2018; Reed et al., 2017). Early studies reported the occurrence of $TiO_2$ engineered nanoparticles in surface waters by measuring the total concentration of Ti using elemental analysis accompanied with $TiO_2$ particle identification by electron microscopy techniques (Peters et al., 2018; Neal et al., 2011). However, these studies did not distinguish between the contributions of natural and engineered particles to the total Ti concentrations. Titanium is the ninth most abundant element in the Earth's crust and is mainly found in minerals such as rutile, ilmenite, sphene, and/or opaque heavy minerals (*e.g.,* titanomagnetite, magnetite, and ilmenite) (Barksdale, 1950). These minerals always contain trace concentrations of other elements (Craigie, 2018). Natural $TiO_2$ minerals, such as rutile and ilmenite, have been shown to be the dominant carriers (*e.g.*, > 90–95% of the whole rock content) of Ti, Nb, Ta, Sb, and W, as well as, important carriers (5–45% if the whole rock content) of V, Cr, Mo, and Sn (Zack et al., 2002). Natural Ti-containing particles form after weathering of parent rocks, and display similar elemental compositions, associations, and ratios as those of the parent rocks. For instance, characterization of naturally occurring Ti-containing particles by single particle-inductively coupled plasma-mass spectrometer (SP-ICP-TOF-MS) demonstrated that natural Ti-particles contain other elements such as Al, Si, Fe, Mn, Ce, La, Zr, Nb, Pb, Ba, Th, Ta, W, and U (Loosli et al., 2019; Gondikas et al., 2018). These natural elemental impurities are typically removed from the natural Ti-containing minerals by dissolution and reprecipitation during the manufacturing of $TiO_2$ engineered particles (Loosli et al., 2019). Therefore, mobilization of $TiO_2$ engineered particles with urban runoff to receiving surface waters will lead to increases in the elemental ratios of Ti to the elements naturally associated with Ti-containing minerals. This approach has been recently implemented to estimate the concentrations of $TiO_2$ engineered particles in sewage spills (Loosli et al., 2019), urban runoff (Wang et al., 2020), and surface waters (Gondikas et al., 2014).

This study builds on previous advancements in overcoming some of the challenges in the detection and quantification of titanium dioxide engineered particles in surface waters (Loosli et al., 2019; Wang et al., 2020; Gondikas et al., 2014, 2018) by evaluating the temporal variability in titanium dioxide engineered particle concentrations in an urban river during and following rainfall events. The aims of this study are to: 1) characterize the elemental composition of Ti-containing particles in the Broad River on a single particle basis using SP-ICP-TOF-MS during and following rainfall events, **2)** monitor the occurrence and concentration of $TiO_2$ engineered particles in the Broad River, and **3)** determine the possible source(s) of $TiO_2$ engineered particles in the Broad River, Columbia, South Carolina, United States.

## 2. Materials and methods

### 2.1. Sampling

Water samples were collected from the Broad River, Columbia, SC 29201 (34°00′10.4″N 81°03′18.4″W, Figure S1). The Broad river is approximately 240 km long, originates in the Blue Ridge Mountains of eastern Buncombe Country, North Carolina, and flows generally south-southeastwardly in South Carolina. The total catchment area of the Broad River is approximately 14,000 square kilometers. The broad River is a principal tributary of the Congaree River, which is a principal tributary of the Santee River, which discharges in the Atlantic Ocean. Apart from the forested land (66%) in the headwaters of the Broad river basin; the dominant land use throughout the Broad river basin is agricultural (23%); urban (9%): commercial and residential; others (2–4%): mining operations, and logging operations. There are 14 permitted major wastewater treatment plants (WWTP), 30 minor WWTPs, 20 animal operation facilities, and 92 general and individual stormwater facilities in the Broad river basin (NC DEQ, 2009).

Water samples were collected from the Broad River during a range of hydrologic conditions (Table S1). The first sampling campaign (C1) was conducted between September 14, 2018 and September 21, 2018 during and following Hurricane Florence, which formed on August 31, 2018, dissipated on September 19, 2018, and made landfall near Wrightsville Beach in North Carolina on September 14th. The hurricane eye moved westward through North Carolina and the Northern part of South Carolina without any significant impact on Columbia, South Carolina. Nonetheless, hurricane Florence generated rainfall in Columbia, SC of a maximum total daily rainfall of 42 mm between September 15th to 18th 2018 (Table S1) (Stewart and Berg, 2019). The second sampling campaign (C2) was performed between October 25, 2018 and November 02, 2018 during which a major rainfall event of a 33 mm occurred on October 26, 2018 (Table S1). The third sampling campaign (C3) was

performed between November 05, 2018 and November 09, 2018 during which low intensity rainfall (0–3.5 mm) occurred on nearly daily basis except on 11/07/208, where a rainfall with higher intensity (19 mm) occurred. The rainfall data was collected from the USGS station number 021695045 (34°00′24″N 81°01′18″W), nearly 3.1 km from the sampling location. The discharge data was collected from the USGS station number 02162035 (34°02′54″N 81°04′24″W), nearly 5.3 km upstream of the sampling location.

### 2.2. Sample collection, digestion and elemental analysis

Surface water samples were collected from the Broad River in 1 L high density polyethylene bottles (Thermo Scientific, Rockwood, TN, United States). Prior to use, bottles were acid-washed in 10% nitric acid (Sigma Aldrich, St. Louis, MO, United States) for at least 24 h, and soaked in ultrahigh purity water (PURELAB Option-Q, ELGA, High Wycombe, UK) for 24 h, air dried, and then double-bagged. In the field, the sampling bottles were rinsed three times in the surface water and then filled with the water sample, samples were individually double-bagged, and returned to the lab the same day and were stored in the dark at 4 °C.

The bulk river water samples were digested in 15 mL Teflon vessels (Savillex, Eden Prairie, MN, United States) on custom-made Teflon covered hotplates placed in a box equipped with double-HEPA filtered forced air in a metal-free HEPA filtered air clean lab. 10 mL water aliquots or 5 mL extracted particle suspensions were placed in the vessel and weighed (Mettler Toledo, Excellence Plus, Columbus, OH, United States). Samples were dried at 110 °C and treated with 1 mL of 30% $H_2O_2$ (Fisher Chemical, Fair Lawn, NJ, United States) for 2 h at 70 °C to remove organic matters. $H_2O_2$ was then evaporated and the sample was digested with 2 mL of HF:$HNO_3$ (3:1) mixture (ACS grade acids distilled in the laboratory, Sigma Aldrich, St. Louis, MO, United States) for 48 h at 110 °C. After evaporation of the acid mixture at 110 °C, the residue was reacted with 1 mL of distilled $HNO_3$ to break up insoluble fluoride salt that may have formed during the sample digestion and $HNO_3$ was left to evaporate at 110 °C. This step was repeated twice before weighing the sample and adding 5 mL of 1% $HNO_3$. The sample was sonicated for 10 min in a sonication bath (Branson, 2800, 40 kHz, Danbury, CT, United States) and warmed for 2 h at 50 °C for full dissolution. The solution was transferred to 15 mL polypropylene centrifuge tubes (Fisher Scientific, San Nicolás de los Garza, Nuevo León, Mexico) and stored at 4 °C. Samples were centrifuged (Eppendorf, 5810 R, Hamburg, Germany) for 5 min at 3100 g prior to ICP-MS analysis to remove any undigested minerals.

The elemental concentrations of the USGS reference materials BHVO-2 Hawaiian basalts run as unknowns after digestion following the digestion procedure described above demonstrate high recovery (approximately 100%) for most elements. The precision of our method was better than 4% for all isotopes except $^{169}$Tm and $^{174}$Lu (7 and 8%) and the accuracy was better than 89% for most elements, including Ti and Nb except $^{174}$Lu (86%). Full procedural digestion blanks was <6.8% for all elements and <2.8% for titanium and niobium of samples' analyte signal (Table S2). Therefore, blanks are insignificant to the calculations of Ti concentrations or total Ti/Nb elemental ratios.

Elemental concentrations in the digested river water samples were determined by PerkinElmer NexION 350D ICP-MS (operating conditions are summarized in Table S3). Standard tuning procedure was performed before analysis for instrument maintenance. Dissolved multi-element standards mixture of ICP Complete Group Calibration Standard (BDH Chemicals, Radnor, PA, USA) and ICP Refractory Element Group Calibration Standard (BDH Chemicals, Radnor, PA, USA) diluted in 1% nitric acid (TraceMetal grade, Fisher Chemical, Fair Lawn, NJ, USA) were used for mass concentration calibration ranging from 0.01 to 1000 μg $L^{-1}$. Internal standards (ICP Internal Element Group Calibration Standard, BDH Chemicals, Radnor, PA, USA) were monitored at the same time for quality control. The isotopes measured were $^{27}$Al, $^{47}$Ti, $^{57}$Fe, $^{93}$Nb, $^{139}$La, $^{140}$Ce, $^{141}$Pr, $^{142}$Nd, $^{152}$Sm, $^{153}$Eu, $^{158}$Gd, $^{159}$Tb, $^{164}$Dy, $^{165}$Ho, $^{166}$Er, $^{169}$Tm, $^{174}$Yb, and $^{175}$Lu. All isotopes were analyzed in standard mode.

### 2.3. Particle composition on single particle basis

The Broad river water samples were shaken well prior extraction to resuspend any settled particles and to obtain a representative subsample. 10 mL aliquots were transferred into acid-washed 15 mL centrifuge tubes. The transferred samples were bath sonicated for 2 h (Branson, Model 2800, 40 kHz, Danbury, CT, United States), then centrifuged at 775 g for 5 min to remove large particles (>1000 nm assuming natural particle density, $\rho = 2.5$ g $cm^{-3}$) in order to prevent clogging of the ICP-TOF-MS introduction system. The top 7 mL supernatant was decanted and stored at 4 °C in the dark till analysis by SP-ICP-TOF-MS. The theoretical size of the extracted suspensions corresponds to particles <1000 nm for natural particles ($\rho = 2.5$ g $cm^{-3}$), and <725 nm for $TiO_2$ particles ($\rho = 4.2$ g $cm^{-3}$). All samples were bath sonicated again for 15 min and were diluted by a factor of 100 prior to SP-ICP-TOF-MS analysis.

Single particle analysis of the diluted particle extracts was performed using an ICP-TOF-MS (TOFWERK, Thun, Switzerland) to determine all isotopes within a single particle simultaneously (operating conditions are summarized in Table S4) (Hendriks et al., 2017). Element specific instrument sensitivities were measured with a multi-element solution mix prepared from a three multi-element solution (0, 1, 2, 5, and 10 μg$L^{-1}$ multi element standard, diluted in 1% $HNO_3$, BDH Chemicals, Radnor, PA, USA) as described above. The transport efficiency was calculated using the known size approach (Pace et al., 2011) using both Au ENMs with a certified particle size of 60 nm (NIST RM8013 Au, Gaithersburg, MD, USA) prepared in UPW and Au standard solutions (0, 1, 2, 5, and 10 μg$L^{-1}$, diluted in 1% HCl, BDH Chemicals, West Chester, PA, USA). Using a standard tuning solution, the ICP-TOF-MS mass spectra were calibrated using $^{18}H_2O^+$, $^{59}Co^+$, $^{115}In^+$, $^{140}Ce^+$, and $^{238}U^+$ target isotopes in TofDAQ view (TOFWERK) prior analysis or in Tofware (TOFWERK) after analysis if mass shifts occurred during analysis. Particle/baseline signal separation, particle signal, mass, and number concentration were determined from mass-calibrated ICP-TOF-MS spectra using Python script in Tofware as described elsewhere (Loosli et al., 2019). The particle detection threshold was calculated for each isotope according to Eq. (1) (Tanner, 2010).

$$\text{Threshold} = \text{Mean} + (3.29\sigma + 2.71) \quad (1)$$

The data for each isotope were treated separately, but the time stamps were kept throughout data processing for every isotope, allowing for identification of isotope correlations in a single particle. For example, an impure particle (*e.g.,* a particle containing multiple elements) generates several isotope signals spikes in a given time stamp. An "apparently pure" particle generates one isotope signal spike in a given time stamp. The term "apparently pure" is used in this study as such particles might contain elements at concentrations below the sp-ICP-MS mass/size detection limit. Elemental association and elemental ratio distributions were determined using data filtration in Excel.

### 2.4. Estimation of $TiO_2$ engineered particle concentration

The concentration of $TiO_2$ engineered particles was calculated

based on mass balance calculations according Eq. 2

$$[TiO_2]_{engineered\ particles} = \frac{TiO_2\ MM}{Ti\ MM}\left[Ti_{sample} - Nb_{sample}\cdot\left(\frac{Ti}{Nb}\right)_{background}\right] \quad (2)$$

where, $[TiO_2]_{engineered\ particles}$ is the concentration of $TiO_2$ engineered particles, Ti $_{MM}$ and $TiO_2$ $_{MM}$ are the molar masses of Ti and $TiO_2$, $Ti_{sample}$ and $Nb_{sample}$ are the concentrations of Ti and Nb in a given sample, $Ti/Nb_{background}$ is the natural background elemental concentration ratio of Ti/Nb. Background Ti/Nb ratio was calculated on eight reference samples collected from Lake Katherine and Gills creek in Columbia, SC in the absence of rainfall events (Loosli et al., 2019).

Eq (2) assumes that all Ti occurs in particulate form, engineered Ti occurs as pure $TiO_2$ engineered particles, and that the natural background elemental ratio of Ti/Nb is constant through the sampling period. These assumptions are justified for the following reasons. Ti is expected to occur solely in solid phases in the Broad River surface water because of the very low solubility of $TiO_2$ (Antignano and Manning, 2008). While Ti has numerous industrial applications, from metal alloying to aerospace applications to biomedical devices, approximately 95% of the mined Ti is refined into nearly pure $TiO_2$ through the treatment of Ti-bearing ores with carbon, chlorine, or sulfuric acid (USGS, 2019). Additionally, $TiO_2$ engineered particle contain trace amount of Nb, which is below the ICP-MS detection limit (*e.g.,* < 7 ng $L^{-1}$) for $TiO_2$ concentrations up to 10,000 mg $L^{-1}$ (Wang et al., 2020). On the other hand, natural $TiO_2$ minerals are the dominant carriers (*e.g.,* > 90–95% of the whole rock content) of Ti and Nb (Zack et al., 2002). The elemental ratio of Ti/Nb, Ti/Fe, and Ti/Al, determined by SP-ICP-TOF-MS, in naturally occurring particles in the Broad River waters were found to be constant throughout the sampling campaigns (*see results and discussion* section 3.4).

### 2.5. Hydrographs and separation of base flow and runoff

The discharge was separated into base flow and direct runoff using "WHAT: Web-based Hydrograph Analysis Tool" (Lim et al., 2005). The base flow and direct runoff separation was performed for the USGS station number 02162035 using the following method and conditions. Method: Recursive digital filter; aquifer type: perennial streams with porous aquifer; filter parameter: 0.98; and $BFI_{max}$: 0.80.

## 3. Results and discussion

### 3.1. Precipitation, hydrograph, and separation of base flow and runoff

Precipitation occurred at the beginning of the first two sampling events and during the third sampling event (Table S1; Figure S2), which resulted in runoff events in the Broad River. Direct runoff accounted for 30–60% of the total discharge during the first event, 15–70% during the second sampling event, and <30% of the total discharge in the 3rd sampling event. It is worth noting that baseline flow (*i.e.,* no urban runoff contribution) occurred on September 21, 2018, October 31, 2018, and November 01, 2018.

### 3.2. Elemental pollutographs

Pollutographs (*i.e.,* graphs of pollutant concentrations *vs.* time) of Ti, Nb, Ce, and La are displayed in Fig. 1 to illustrate their transport pathways in the Broad River during rainfall events. Ti, Nb, Ce, and La exhibited a mobility pattern driven by the transport of solids (Galfi et al., 2017). At the start of the hydrographs, during low flows, concentrations were rather low, increased with increasing flow (transporting more solids) and then declined with diminishing flow and supply of solids on the catchment surfaces (Fig. 1). This suggests that urban runoff contributes a major Ti, Nb, Ce, and La loads to the Broad River. During the first sampling campaign (C1), Ti reached a maximum value of 108 ± 4.5 μg $L^{-1}$, which coincided with the discharge and runoff peaks, then decreased to 36 ± 0.4 μg $L^{-1}$ with decreasing discharge (Fig. 1a). The lowest Ti concentration coincided with the decrease in runoff to zero on September 21, 2018 (Figure S2). During the second sampling event (C2), the Ti concentration varied between 53 ± 0.5 to 298 ± 6 μg $L^{-1}$ (Fig. 1). The lowest Ti concentration during C2 was observed prior to the runoff peak as this event was preceded by 13 days dry period. The highest Ti concentration during C2 coincided with the second peak of the discharge. During the third sampling event (C3), the lowest Ti concentration was 47.9 ± 6.0 μg $L^{-1}$ and coincided with the lowest discharge and lowest runoff (*e.g.,* 14% of the total discharge). Overall, the highest Ti concentration was measured during the second sampling event due to the long antecedent dry period which might have resulted in higher contaminant accumulation on impervious surfaces in the watershed. Similar increases in the concentrations of particulate matter associated contaminants (*e.g.,* metals) with increases in antecedent dry period was observed for road runoff (Tian et al., 2009; Yuan et al., 2017). The maximum Ti concentrations measured in C1 and C3 were lower than that measured in C2, possibly due to short antecedent dry period (2days) and dilutional effect in C1, and the absence of antecedent dry period in C3. These short antecedent dry periods prior to C1 and the absence of antecedent dry period in C3 results in lower contaminant accumulation on impervious surfaces in the watershed.

Unlike other sources of pollutants, such as municipal or industrial wastewaters, where the sources of titanium-containing particles are predominantly anthropogenic in nature (Kiser et al., 2009), significant quantities of titanium-containing particles occur in urban runoff as a result of soil erosion and atmospheric deposition of soil particles on surfaces in the urban environment (Pereira et al., 2007). Therefore, the differences in the total Ti concentration in the river stream during rainfall events can be attributed to the differences in natural and/or engineered Ti concentrations. The differences in the natural Ti concentration can be affected by the difference in natural sources of sediments to the river, *i.e.* erosion of soils, channel banks, and floodplain deposits; atmospheric dust deposition; landslides; and debris flows *etc*. The differences in the engineered Ti concentrations can be impacted by the difference in sources of $TiO_2$ to the river, *i.e.* sunscreens (Gondikas et al., 2014; Reed et al., 2017), urban runoff (Wang et al., 2020), wastewater treatment plant (WWTP) effluent (Kiser et al., 2009), or sanitary sewage overflows (Loosli et al., 2019).

### 3.3. Elemental ratio profiles

All rainfall events resulted in higher Ti/Nb ratios than the average water reference samples collected in nearby water bodies (266 ± 9) and to the average crustal value (320) (Fig. 2) (Loosli et al., 2019). The lowest Ti/Nb ratio of 330 ± 5 was measured on October 31, 2018, where the river discharge was mainly baseflow (Figure S2) and the highest Ti/Nb ratio of 565 ± 1 was measured during C1 on September 18, 2018, on which the direct runoff was higher than the baseflow (Figure S2). The lower Ti/Nb ratios observed during C2 might be attributed to the higher proportion of naturally occurring particles compared to engineered particles in urban runoff during C2 due to the long antecedent dry period (Schiff and Tiefenthaler,

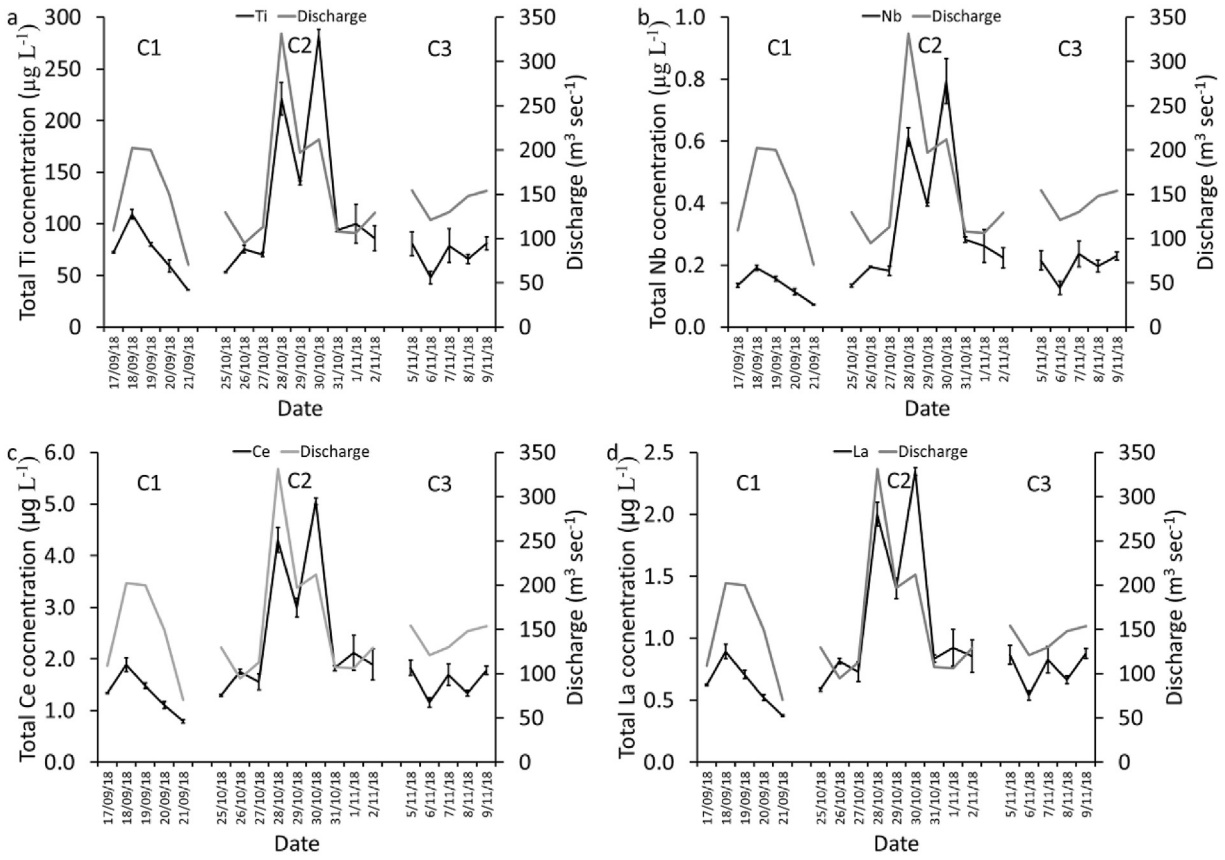


**Fig. 1.** Pollutographs (*i.e.,* graphs of pollutant concentrations *vs.* time) of (a) Ti, (b) Nb, (c) Ce, and (d) La in the Broad River water during the three sampling campaigns.

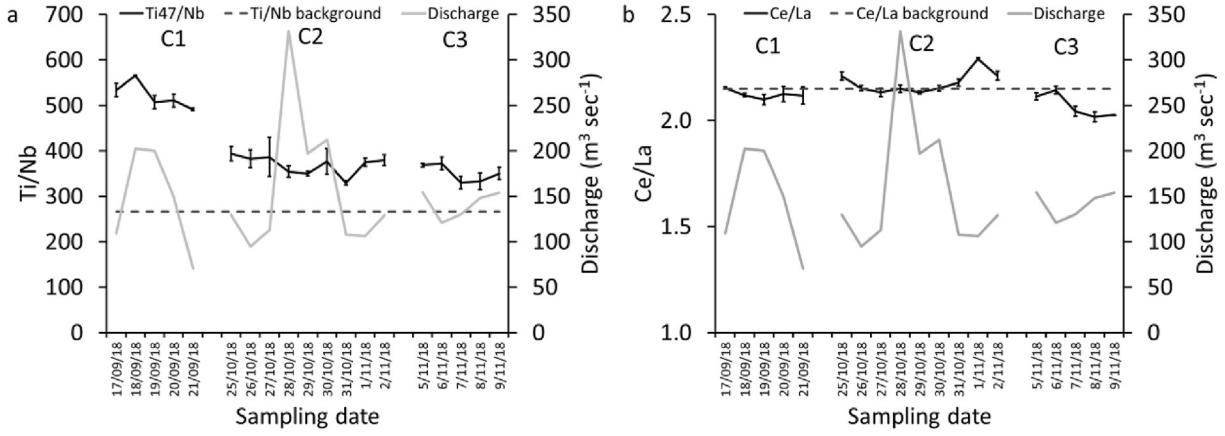


**Fig. 2.** Elemental ratios of (a) Ti/Nb and (b) Ce/La in the Broad River bulk water samples during the three sampling campaigns. The background Ti/Nb and Ce/La ratios are average ratios of eight water samples collected in from water bodies near the sampling site in the absence of rainfall events.

2001). Ti/Nb was generally low during C3, which might be attributed to the absence of antecedent dry period and the continuous low intensity rainfall, and thus the low input of engineered Ti to the Broad River. In contrast to the variation in Ti/Nb ratios, the elemental ratios of Ce/La varied within a narrow range (2.0 ± 0.02 to 2.3 ± 0.01) throughout the three sampling campaigns (Fig. 2b), which is very close to the average crustal Ce/La ratio (2.13) and the average background water Ce/La (2.15 ± 0.01) ratio near the sampling sites (Loosli et al., 2019), indicating the absence of Ce and La contamination, as well as, the accuracy of the digestion and analysis procedure used in this study. The nearly constant Ce/La ratio and the high concentration of Ce and La in the Broad River water during rainfall events indicate a significant introduction of natural particles with the urban runoff to the Broad River.

Given the significant contribution of natural particles to urban runoff as indicated by the high Ce and La concentrations, the differences in the Ti/Nb elemental ratios in the bulk water samples can be attributed to 1) variability in the elemental ratios within natural occurring Ti-containing particles, or **2)** the introduction of $TiO_2$ engineered particles which do not contain Nb (Baalousha et al., 2020). The strong association between Ti and Nb in titanium minerals (Craigie, 2018; Zack et al., 2002; José and Wyllie, 1983)

suggests that these variations are due to $TiO_2$ engineered particles contamination. To further confirm this hypothesis the elemental associations and the variability in Ti/tracer in Ti-containing particles were investigated by SP-ICP-TOF-MS.

### 3.4. Particle number concentration and elemental composition

The number concentration of Ti-, Nb-, Ce-, and La-containing particles (Fig. 3) followed the same trend as the corresponding total element concentration in the bulk water (Fig. 1). Fourteen major and trace elements were detected in Ti-containing particles including Al, Si, V, Mn, Fe, Ni, Zr, Nb, Ba, Ce, La, Pb, and Th. These findings are in agreement with elemental associations between Ti and natural tracers observed in surface waters (Loosli et al., 2019) and soils (data not published yet) in South Carolina as well as with occurrence of these elements in $TiO_2$ natural phases (*e.g.,* rutile, ilmenite, etc.) (Craigie, 2018; Zack et al., 2002; José and Wyllie, 1983). Natural $TiO_2$ minerals, such as rutile and ilmenite, have been shown to be the dominant carrier (*e.g.,* > 90–95% of the whole rock content) for Ti, Nb, Ta, Sb, and W as well as an important carrier (*e.g.,* 5–45% of the whole rock content) for V, Cr, Mo, and Sn in $TiO_2$-bearing metamorphic rocks (Zack et al., 2002). All the elements detected in Ti-containing particles by SP-ICP-TOF-MS, except Nb, occurred in association with Ti as well as free of Ti. Nb was the only element that occurred only in association with Ti- containing particles, further confirming the strong association between Ti and Nb in natural particles. Therefore, Ti/Nb in the digested samples was used to differentiate natural from engineered Ti-containing particles and quantify the concentrations of $TiO_2$ engineered particles in the Broad River during and following different rainfall events.

The elemental ratio distributions of Ti/Nb, Ti/Al, and Ti/Fe in Ti-containing particles displayed the same trend in all samples (Fig. 4), indicating that naturally occurring Ti-containing particles were not different between the different samples. Particles containing Ti and Nb displayed Ti/Nb ratios between 20 and 400, with only a small fraction (<10%) of particles with Ti/Nb ratios > 400 (Fig. 4a). The mean elemental ratio of Ti/Nb varied between 66 ± 49 to 242 ± 247 (standard deviation here is that of the Ti/Nb distribution), lower than the average crustal values (*e.g.,* 320) and the average value measured in reference water samples collected in Columbia, SC (*e.g.,* 266 ± 9). The variability in the Ti/Nb elemental ratios between the different samples can be attributed to the detection of a small number (4–110 particles) of the particles containing both Ti and Nb. Only few particles containing both Ti and Nb were detected by sp-ICP-TOF-MS because of the mass/size detection limit of SP-ICP-TOF-MS (*e.g.,* 30–35 nm under the current experimental conditions) and the low concentration of Nb in Ti-containing particles

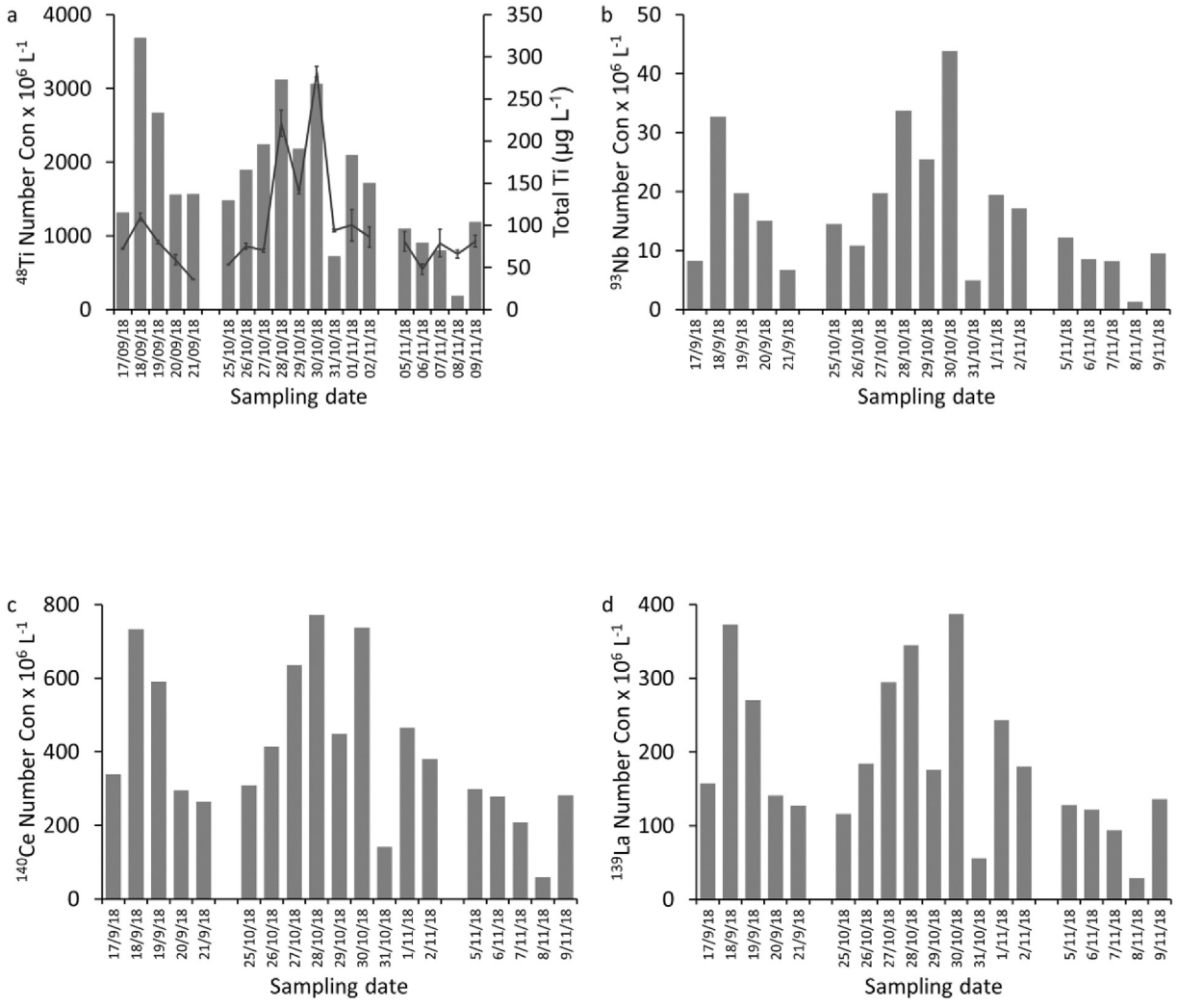


**Fig. 3.** Number concentration of (a) Ti-, (b) Nb-, (c) Ce- and (d) La-containing particles in the Broad River water during the three sampling campaigns.

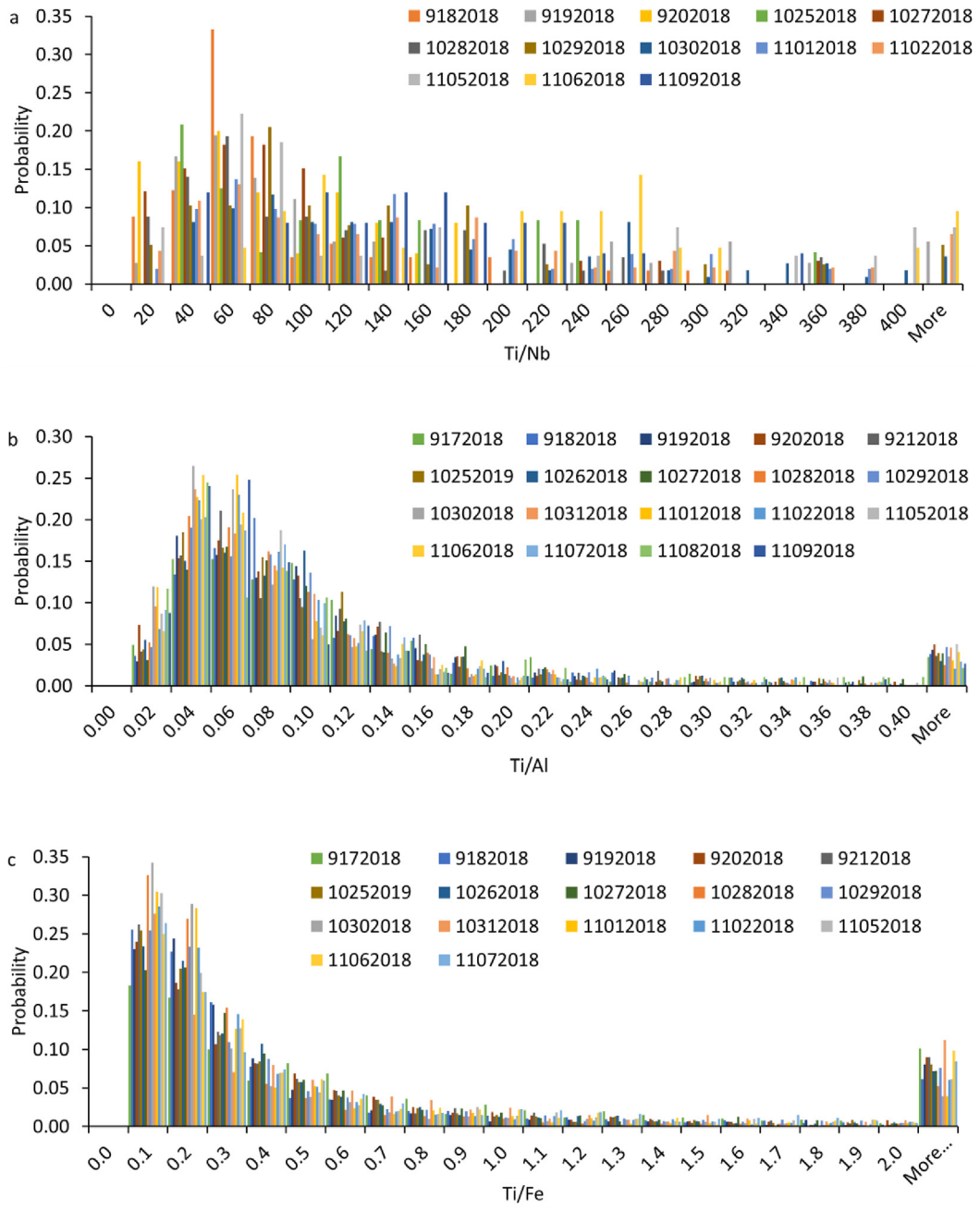


**Fig. 4.** Elemental ratio distributions of (a) Ti/Nb, (b) Ti/Al, and (c) Ti/Fe in Ti-containing particles on a single particle basis measured by single particle-inductively coupled plasma-time of flight-mass spectrometer (SP-ICP-TOF-MS). For Ti/Nb, only samples that contained at least 20 particles containing Ti- and Nb-are presented in panel a.

(*e.g.,* 20–400 times lower than Ti, Fig. 4a). On the other hand, significantly higher number of particles containing both Ti and Al (91–773) and Ti and Fe (325–1688) containing particles were detected by SP-ICP-TOF-MS. This is because Al and Fe concentrations in Ti-containing particles are higher than Nb. The higher number of Ti- and Fe-containing particles compared to Ti- and Al-containing particles is due to the lower size detection limit of Fe (*e.g.,* 44–65 nm under the current experimental conditions) compared to Al (*e.g.,* 138–170 nm under the current experimental conditions). Therefore, a comparison of the elemental ratios of Ti/Al and Ti/Fe among the different samples was used to evaluate if naturally occurring particles were different during the sampling events.

The elemental ratios of Ti/Al display the same distribution in all samples (Fig. 4b). These elemental ratios are in good agreement with naturally occurring particles such as palygorskite and montmorillonite (Ti/Al = 0.014–0.016); illite (Ti/Al = 0.026); kaolinite and hectorite (Ti/Al = 0.06); vermiculite and corrensite (Ti/Al = 0.090–0.093). Similarly, the elemental ratios of Ti/Fe display the same distribution in all samples (Fig. 4c) and are in good agreement with natural occurring titanium minerals such as titanomagnetite ($Fe_{3-x}Ti_xO_4$, $0 < Ti/Fe < 0.43$, $0 < x < 1$), ulvöspinel ($Fe_2TiO_4$, Ti/Fe = 0.43), pseudobrookite ($Fe_2TiO_5$, Ti/Fe = 0.43), ilmenite ($FeTiO_3$, Ti/Fe = 0.86), pseudorutile ($Fe_2Ti_3O_9$, Ti/Fe = 1.29), and ilmenorutile and ferropseudobrookite ($FeTi_2O_5$, Ti/Fe = 1.71).

Collectively these results indicate that the elemental ratios of Ti/Nb, Ti/Al, and Ti/Fe in naturally occurring Ti-containing particles were similar between the different samples. Therefore, there was no variability in natural occurring particles during the sampling period. Thus, any changes in total elemental ratios can be attributed to the occurrence of titanium oxide engineered particles in these samples.

### 3.5. $TiO_2$ concentrations and sources

The calculated $TiO_2$ engineered particle concentrations based on shifts in Ti/Nb elemental ratios varied between 21 ± 5 μg $L^{-1}$ and 143 ± 22 μg $L^{-1}$ and followed the same trend of rise and fall as the discharge/direct runoff (Fig. 5). The highest $TiO_2$ concentration was found in the second sampling campaign, likely due to the long antecedent dry period (13 days) prior to the sampling campaign in comparison to the other sampling campaigns. The occurrence of $TiO_2$ engineered particles in high concentrations in the Broad River stream is in good agreement with the extensive use of $TiO_2$ engineered particles in the urban environment as engineered nanoparticles in self-cleaning and photocatalytic surfaces and as pigment in paint and coatings (Chemours, 2018; Shandilya et al., 2015) which have been shown to be released by wear and weathering (Nored et al., 2018); and the occurrence of $TiO_2$ engineered particles in road dust, atmospheric particulate matter (Lee et al., 2016; Wilczynska-Michalik et al., 2014), urban runoff (Wang et al., 2020), and WWTPs effluent (Westerhoff et al., 2011). The $TiO_2$ concentrations measured in this study are much higher than the predicted $TiO_2$ engineered particle concentrations in surface waters (0.0002–24.5 μg $L^{-1}$) and the measured $TiO_2$ engineered particle concentrations in river waters (0.55–6.5 μg $L^{-1}$) (Markus et al., 2018; Donovan et al., 2016; Neal et al., 2011).

$TiO_2$ engineered particles enter surface waters from different sources such as effluent of wastewater treatment plants (WWTP), sanitary sewage overflows, urban runoff, industrial discharge, or construction activities. Gadolinium anomaly is widely used to track effluent from wastewater treatment plants (Verplanck et al., 2010). Gadolinium anomalies >1.5 has been used as an indicator of wastewater treatment effluent in river waters. The size of gadolinium anomaly throughout the sampling events was <1.2 (Figure S4b), indicating the absence of WWTP effluent or sewage spills. There were no construction activities near the sampling site. There are no known industrial discharge sources near the sampling location. Furthermore, both industrial and construction activities would result in a continuous discharge of $TiO_2$ particles to surface water. However, the observed Ti-contamination in this study was correlated/in response to rainfall events, suggesting that the source of $TiO_2$ particles here is urban runoff.

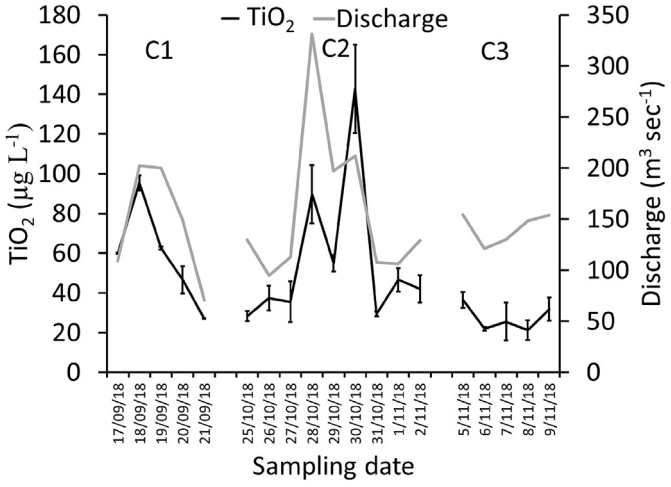


**Fig. 5.** The calculated $TiO_2$ concentrations in the Broad River water during the three sampling campaigns.

## 4. Analytical and environmental perspectives

Characterization and quantification of engineered particles in Rivers draining large watersheds is challenging. Identifying the natural background of elemental ratio of Ti/Nb is quite complicated for large urban rivers such as the Broad River. This is because there are many sources of $TiO_2$ engineered particles release to surface waters in large urban rivers such as urban runoff, sewage spills, wastewater treatment effluent, and resuspension of contaminated sediment (Loosli et al., 2019; Galfi et al., 2017; Horowitz et al., 2008). For instance, there are 44 WWTPs upstream of the sampling site contributing a total of 144 × $10^3$ $m^3$ of effluent discharge per day (NC DEQ, 2009) Atmospheric particles released within the urban environment can also deposit on the water surface in the Broad River. Additionally, engineered particles could be introduced to the Broad River with urban runoff upstream of the sampling site due to the large watershed area. Even during a dry day near the sampling location, a rainfall event upstream will deliver contaminants, including engineered particles, into the sampling location. The continuous introduction of $TiO_2$ engineered particles into surface waters result in a shift in the natural background elemental ratios toward higher values. The lowest elemental ratio of Ti/Nb in the Broad River in the absence of direct runoff was 330 ± 5, which was higher than the reference value (*e.g.,* 266 ± 9) measured in smaller creeks in the sampling area and in a rural river in South Carolina monitored for the occurrence and concentrations of $TiO_2$ engineered particles over a period of two years (data not published yet). The selection of the incorrect background elemental ratio (*e.g.,* at the beginning or the end of the event hydrograph) will results in the underestimation of $TiO_2$ engineered particles. This requires long term monitoring of the site(s) under consideration to achieve the true (lowest) elemental ratio baseline value. Furthermore, monitoring the concentration of $TiO_2$ engineered particles in smaller river reaches with fewer potential sources of $TiO_2$ engineered particles might be useful to better understand the processes determining the fate and transport of $TiO_2$ engineered particles in surface waters.

Here we reported the concentrations of $TiO_2$ engineered particles in the Broad River following rainfall events. The $TiO_2$ concentrations varied between 20 and 140 μg $L^{-1}$ during the sampled events. These concentrations are in the same order of magnitude as the predicted no effect concentration (PNEC) for $TiO_2$ pigments (*e.g.,* 127–184 μg $L^{-1}$) and is higher than the PNEC for $TiO_2$ ENMs to freshwater organisms (*e.g.,* 1–18 μg $L^{-1}$) (Mueller and Nowack, 2008; Lützhøft et al., 2015). Transport of $TiO_2$ engineered particles with river water to the ocean could also pose a significant risk for coral reefs. $TiO_2$ engineered particles have been shown to bioaccumulate in microflora and induce coral bleaching, which could contribute to an overall decrease in coral populations (Jovanovic and Guzman, 2014). Further research is needed to further understand the impact of rainfall characteristics and the hydrogeological factors on the temporal variability in $TiO_2$ engineered particle concentrations in urban rivers.

## 5. Conclusion

This study reports the measurement of $TiO_2$ engineered particle concentrations in the Broad River, Columbia, South Carolina, United States following rainfall events. The concentration of $TiO_2$

engineered particle were estimated by mass balance calculations using total titanium concentrations and increases in Ti/Nb ratios above the natural background ratios. The elemental ratios of Ti/Nb (*e.g.,* 330 to 565) were higher than the average crustal values (*e.g.,* 320) and the natural background elemental ratios in surface waters in Columbia, SC (*e.g.,* 266 ± 9) and followed the same trend of rise and fall as the discharge/runoff, suggesting introduction of $TiO_2$ engineered particle to the Broad River water with urban runoff. The concentrations of titanium dioxide engineered particles in the Broad River varied between 20 and 140 μg $TiO_2$ $L^{-1}$ following rainfall events. Such high concentrations of $TiO_2$ engineered particles to urban rivers may pose environmental risks during and following rainfall events. This study highlights the importance of determining the temporal variations in engineered particle concentrations in surface waters for a more comprehensive understanding of the environmental fate, behavior, and risk assessment of engineered particles.

## Author contributions section

Dr. Baalousha conceived the overall idea of the study. Mr. Nabi and Dr. Wang performed all experimental and data analysis. All authors contributed to writing, proof reading, and revision of the manuscript.

## Declaration of competing interest

The authors declare that they have no known competing financial interests or personal relationships that could have appeared to influence the work reported in this paper.

## Acknowledgment

This work was supported by US National Science Foundation CAREER (1553909) grant to Dr. Mohammed Baalousha, and by funding from the University of South Carolina, Office of Research (13020-19-51236).

## Appendix A. Supplementary data

Supplementary data to this article can be found online at https://doi.org/10.1016/j.chemosphere.2020.128261.

## References

Antignano, A., Manning, C.E., 2008. Rutile solubility in H2O, H2O−SiO2, and H2O−NaAlSi3O8 fluids at 0.7−2.0 GPa and 700−1000 °C: implications for mobility of nominally insoluble elements. Chem. Geol. 255, 283−293.

Baalousha, M., Yang, Y., Vance, M.E., Colman, B.P., McNeal, S., Xu, J., Blaszczak, J., Steele, M., Bernhardt, E., Hochella JR., M.F., 2016. Outdoor urban nanomaterials: the emergence of a new, integrated, and critical field of study. Sci.Tot.Environ. 557−558, 740−753.

Baalousha, M., Wang, J., Mahmudun Nabi, M., Loosli, F., Valenca, R., Mohanty, S.K., Afrooz, N., Cantando, E., Aich, N., 2020. Stormwater green infrastructures retain high concentrations of TiO2 engineered (nano)-particles. J. Hazard Mater. 392, 122335.

Barksdale, J., 1950. Titanium, its occurrence, chemistry, and technology. Soil Sci. 70, 414.

Craigie, N., 2018. Principles of Elemental Chemostratigraphy: a Practical User Guide. Springer International Publishing, Cham, Switzerland.

Donovan, A.R., Adams, C.D., Ma, Y., Stephan, C., Eichholz, T., Shi, H., 2016. Single particle ICP-MS characterization of titanium dioxide, silver, and gold nanoparticles during drinking water treatment. Chemosphere 144, 148−153.

Galfi, H., Österlund, H., Marsalek, J., Viklande, M., 2017. Mineral and anthropogenic indicator inorganics in urban stormwater and snowmelt runoff: sources and mobility patterns. Water, Air, Soil Pollut. 228, 1−18.

Gohler, D., Stintz, M., Hillemann, L., Vorbau, M., 2010. Characterization of nanoparticle release from surface coatings by the simulation of a sanding process. Ann. Occup. Hyg. 54, 615−624.

Gondikas, A., von der Kammer, F., Kaegi, R., Borovinskaya, O., Neubauer, E., Navratilova, J., Praetorius, A., Cornelis, G., Hofmann, T., 2018. Where is the nano? Analytical approaches for the detection and quantification of TiO2 engineered nanoparticles in surface waters. Environ.Sci.Nano. 5, 313−326.

Gondikas, A.P., von der Kammer, F., Reed, R.B., Wagner, S., Ranville, J.F., Hofmann, T., 2014. Release of TiO2 nanoparticles from sunscreens into surface waters: a one-year survey at the Old Danube recreational lake. Environ. Sci. Technol. 48, 5415−5422.

Hendriks, L., Gundlach-Graham, A., Hattendorf, B., Günther, D., 2017. Characterization of a new ICP-TOFMS instrument with continuous and discrete introduction of solutions. J. Anal. Atomic Spectrom. 32, 548−561.

Horowitz, A.J., Elrick, K.A., Smith, J.J., 2008. Monitoring urban impacts on suspended sediment, trace element, and nutrient fluxes within the City of Atlanta, Georgia, USA: program design, methodological considerations, and initial results. Hydrol.Process.An Int.J. 22, 1473−1496.

José, C.G., Wyllie, P.J., 1983. Ilmenite (high Mg, Mn, Nb) in the carbonatites from the Jacupiranga complex, Brazil. Am. Mineral. 68, 960−971.

Jovanovic, B., Guzman, H.M., 2014. Effects of titanium dioxide (TiO2) nanoparticles on caribbean reef−building coral (Montastraea faveolata). Environ. Toxicol. Chem. 33, 1346−1353.

Kiser, M.A., Westerhoff, P., Benn, T., Wang, Y., Perez-Rivera, J., Hristovski, K., 2009. Titanium nanomaterial removal and release from wastewater treatment plants. Environ. Sci. Technol. 43, 6757−6763.

Koponen, I.K., Jensen, K.A., Schneider, T., 2011. Comparison of dust released from sanding conventional and nanoparticle-doped wall and wood coatings. J. Expo. Sci. Environ. Epidemiol. 21, 408−418.

Lee, P.K., Yu, S., Chang, H.J., Cho, H.Y., Kang, M.J., Chae, B.G., 2016. Lead chromate detected as a source of atmospheric Pb and Cr (VI) pollution. Sci. Rep. 6, 36088.

Lim, K.J., Engel, B.A., Tang, Z., Choi, J., Kim, K.-S., Muthukrishnan, S., Tripathy, D., 2005. Automated web GIS based hydrograph analysis tool, WHAT. J. Am. Water Resour. Assoc. 41, 1407−1416.

Loosli, F., Wang, J., Rothenberg, S., Bizimis, M., Winkler, C., Borovinskaya, O., Flamigni, L., Baalousha, M., 2019. Sewage spills are a major source of engineered titanium dioxide release into the environment. Environ.Sci.Nano. 6, 763−777.

Markus, A.A., Krystek, P., Tromp, P.C., Parsons, J.R., Roex, E.W.M., Voogt, P.d., Laane, R.W.P.M., 2018. Determination of metal-based nanoparticles in the river Dommel in The Netherlands via ultrafiltration, HR-ICP-MS and SEM. Sci.Tot.Environ. 631−632, 485−495.

Mueller, N.C., Nowack, B., 2008. Exposure modeling of engineered nanoparticles in the environment. Environ. Sci. Technol. 42, 4447−4453.

Müller, A., Österlund, H., Marsalek, J., Viklander, M., 2020. The pollution conveyed by urban runoff: a review of sources. Sci.Tot.Environ. 709, 136125.

Neal, C., Jarvie, H., Rowland, P., Lawler, A., Sleep, D., Scholefield, P., 2011. Titanium in UK rural, agricultural and urban/industrial rivers: geogenic and anthropogenic colloidal/sub-colloidal sources and the significance of within-river retention. Sci.Tot.Environ. 409, 1843−1853.

Nored, A.W., Chalbot, M.C., Kavouras, I.G., 2018. Characterization of paint dust aerosol generated from mechanical abrasion of TiO2-containing paints. J. Occup. Environ. Hyg. 15, 629−640.

Pace, H.E., Rogers, N.J., Jarolimek, C., Coleman, V.A., Higgins, C.P., Ranville, J.F., 2011. Determining transport efficiency for the purpose of counting and sizing nanoparticles via single particle inductively coupled plasma mass spectrometry. Anal. Chem. 83, 9361−9369.

Parker, N., Keller, A.A., 2019. Variation in regional risk of engineered nanoparticles: nanoTiO2 as a case study. Environ.Sci.Nano. 6, 444−455.

Pereira, E., Baptista-Neto, J.A., Smith, B.J., McAllister, J.J., 2007. The contribution of heavy metal pollution derived from highway runoff to Guanabara Bay sediments - rio de Janeiro/Brazil. An.Acad.Bras.Cienc. 79, 739−750.

Peters, R.J., van Bemmel, G., Milani, N.B., den Hertog, G.C.U., ndas, A.K., van der Lee, M., Bouwmeester, H., 2018. Detection of nanoparticles in Dutch surface waters. Sci.Tot.Environ. 621, 210−218.

Reed, R.B., Martin, D.P., Bednar, A.J., Montano, M.D., Westerhoff, P., Ranville, J.F., 2017. Multi-day diurnal measurements of Ti-containing nanoparticle and organic sunscreen chemical release during recreational use of a natural surface water. Environ.Sci.Nano. 4, 69−77.

Schiff, K.C., Tiefenthaler, L.L., 2001. Anthropogenic versus natural mass emissions from an urban watershed. Southern California coastal water research project, annual report, long Beach California USA. In: WeisbergS, Elmore, D. (Eds.), Southern California Coastal Water Research Project Annual Report 1999-2000. Southern California Coastal Water Research Project, Westminster, CA, pp. 63−70.

Shandilya, N., Le Bihan, O., Bressot, C., Morgeneyer, M., 2015. Emission of titanium dioxide nanoparticles from building materials to the environment by wear and weather. Environ. Sci. Technol. 49, 2163−2170.

Tanner, M., 2010. Shorter signals for improved signal to noise ratio, the influence of Poisson distribution. J.Anal.Atom.Spectrom. 25, 405−407.

Tian, P., Li, Y., Yang, Z., 2009. Effect of rainfall and antecedent dry periods on heavy metal loading of sediments on urban roads. Front. Earth Sci. China 3, 297−302.

Verplanck, P.L., Furlong, E.T., Gray, J.L., Phillips, P.J., Wolf, R.E., Esposito, K., 2010. Evaluating the behavior of gadolinium and other rare Earth elements through large metropolitan sewage treatment plants. Environ. Sci. Technol. 44, 3876−3882.

Wang, J., Nabi, M.M., Mohanty, S.K., Afrooz, A.N., Cantando, E., Aich, N., Baalousha, M., 2020. Detection and quantification of engineered particles in urban runoff. Chemosphere 248, 126070.

Westerhoff, P., Song, G., Hristovski, K., Kiser, M.A., 2011. Occurrence and removal of titanium at full scale wastewater treatment plants: implications for TiO2

nanomaterials. J. Environ. Monit. 13, 1195–1203.
Wilczynska-Michalik, W., Rzeznikiewicz, K., Pietras, B., Michalik, M., 2014. Fine and ultrafine TiO2 particles in aerosol in Krakow (Poland). Mineralogia 45, 65–77.
Yuan, Q., Guerra, H., Kim, Y., 2017. An investigation of the relationships between rainfall conditions and pollutant wash-off from the paved road. Water 9, 232.
Zack, T., Kronz, A., Foley, S.F., Rivers, T., 2002. Trace element abundances in rutiles from eclogites and associated garnet mica schists. Chem. Geol. 184, 97–122.